

# High Energy Deuteron Emission in NX2 Plasma Focus

Mahmud V. Roshan, Rajdeep S. Rawat, Alireza Talebitaher, Rishi Verma,  
Paul Lee, Stuart V. Springham

*National Institute of education, Nanyang Technological University, Singapore*

(Received: 31 August 2008 / Accepted: 6 December 2008)

Nuclear activation of low-Z targets by energetic ions provides an unambiguous diagnostic for the study of ion beams emitted from pulsed plasma devices. In this work, a graphite target was bombarded by high energy deuterons in a plasma focus device with stored bank energy of 2.2 kJ, operated at 1 Hz repetition rate, and at varying gas pressures. The induced activity of  $^{13}\text{N}$  (a  $\beta^+$  emitter) was determined by measuring the 511 keV annihilation gamma-rays with a BGO scintillation detector. The gamma-ray detection efficiency was determined by Monte Carlo simulation. The relevant nuclear reaction for the target activation is  $^{12}\text{C}(d,n)^{13}\text{N}$ , which has a threshold energy of 328 keV. Hence the graphite activation is caused by the high energy tail of the deuteron energy distribution. The highest  $^{13}\text{N}$  yield was obtained for 5.5 mbar deuterium filling pressure. The number of deuterons incident on the graphite was estimated using the thick-target-yield and an assumed energy spectrum of the form  $dN_d/dE \propto E^{-n}$ . The average number of high energy deuterons per shot was found to be  $N_d \approx 2.4 \times 10^{12}$ . The total energy of the deuteron beam is estimated to be 0.25 J which represents a conversion efficiency of about 0.01% from the stored bank energy.

Keywords: plasma focus, deuteron energy, activation method, thick target yield, MCNPX

## 1. Introduction

Plasma focus devices produce a dense magnetically compressed plasma from which several radiations are emitted. The device consists of two coaxial cylindrical electrodes in a gas filled chamber connected, via a high voltage switch, to a capacitor bank. When the high voltage is applied across the electrodes, breakdown of the gas occurs across an insulator sleeve and current flows. The magnetically driven current sheath is accelerated along the device axis towards the open end of the electrodes. Finally, the current sheath sweeps around the end of the inner electrode due to the radial inward  $J \times B$  force. The sheath then collapses radially with azimuthal symmetry. At the time of maximum compression (pinch phase), a hot and dense magnetized plasma column is formed. This pinch column is a strong source of energetic electron and ion beams.

The plasma focus can be operated so as to produce strong electric fields resulting in the acceleration of electrons and ions to many times the capacitor bank charging voltage [1]. A number of models for the acceleration mechanism have been proposed, including compressional heating in the neck of  $m = 0$  instability [2], the influence of anomalous resistance [3], and fast magneto-sonic shock waves [4]. The mechanism of ion beam generation is yet to be satisfactorily explained, despite the large number of studies which have been conducted at many laboratories.

Measurements of plasma focus ion beam energy have employed a variety of techniques including nuclear activation [5], nuclear emulsion [6], solid state nuclear

track detectors [7], Faraday cups [8], and magnetic spectrometers [9]. The measurement of ion energy distribution is important for understanding the behavior of ions in the pinch column and to explain the production of D-D fusion neutrons in detail. Also the energetic plasma focus ion beam has potential for application as an intense pulsed ion source in various fields.

In the present work the activation of a graphite target was used to investigate the deuteron energy distribution in NX2 plasma focus.

## 2. Experimental Setup

The NX2 is a high repetition rate (up to 16 Hz) small Mather-type plasma focus machine with four energy bank modules, Fig 1.

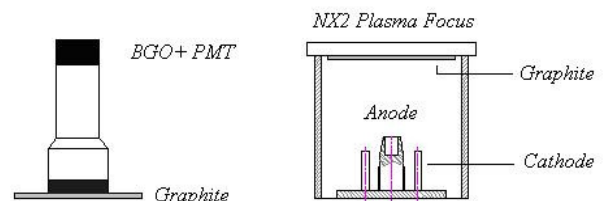


Figure 1. Schematic diagram of NX2 plasma focus and geometry for graphite activation

The hollow copper anode has an effective length of 40 mm and diameter of 23 mm, with a Pyrex glass tube insulating the anode from the base plate and cathode.

This insulator plays an important role in ensuring the symmetry of the initial gas breakdown and current sheath formation. The coaxial cathode comprises 8 copper rods arranged in a squirrel cage configuration. Energy storage is provided by 27.6  $\mu\text{F}$  capacitors coupled to the PF electrodes through four pseudo-spark switches. The total system inductance is 26 nH. When operated with pure  $\text{D}_2$  filling gas, the neutron optimized regime corresponds to a gas pressure of 14 mbar and a charging voltage of 12.5 kV.

Figure 2 shows the typical discharge current derivative,  $dI/dt$ , of the NX2 plasma focus for 5.5 mbar optimum pressure for producing energetic deuterons. The current sheath moves less rapidly when the pressure is increased. Lee's model [10] has been applied to the analysis of the voltage and current traces obtained for these operating conditions. The main parameters resulting from this analysis are: plasma pinch column dimensions of 2 mm diameter and 11 mm length, pinch duration of 70 ns, plasma pinch temperature of 0.5 keV, peak circuit current of 300 kA, and a peak pinch current of 190 kA. The number density of the deuterons given by Bennett equilibrium [11] in the pinch is  $1.9 \times 10^{19} \text{ cm}^{-3}$ .

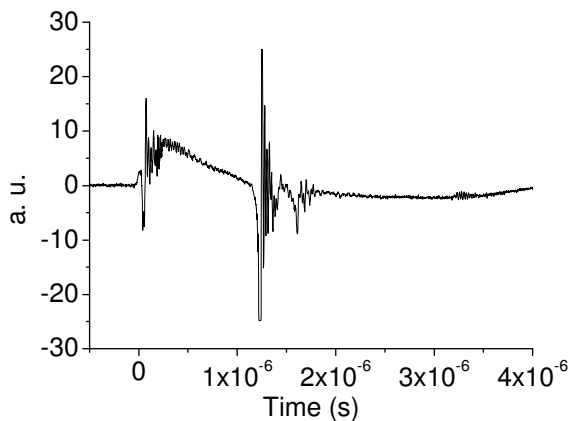


Figure 2. Typical current derivative of NX2 plasma focus (5.5 mbar deuterium)

The graphite target ( $15 \times 15 \text{ cm}^2$ ) was placed normal to the deuteron beam as shown in Fig. 1. The distance between deuteron source (pinch) and the graphite is 100 mm. After a series of shots (30 shots with a repetition rate of 1 Hz), it was then quickly removed from the plasma focus and placed in contact with BGO gamma ray detector to measure the induced activity by the accelerated deuterons produced in the compressed plasma column.

### 3. Results and Discussion

The bombardment of the graphite target by energetic deuterons produces radioactive  $^{13}\text{N}$  via the reaction:



where  $Q = -0.28 \text{ MeV}$ . The threshold energy for the reaction is 328 keV, although the cross-section remains very small below 600 keV. The graphite activation is therefore caused by the high energy tail of the deuteron distribution. The emission of intense high energy deuteron beams is favored in the so-called hard X-ray regime. A strong correlation is observed between the intensity of high-energy deuterons and the intensity of hard X-ray (HXR) pulse. This is because HXR production is due to the bombardment of the anode by high energy electrons, and it is likely that the same mechanism governs ion and electron acceleration [12].

Deuterium-fill pressure has the greatest effect on the yield of high-energy deuterons which is reflected in the number of gamma counts in the spectrum measured with the BGO scintillation detector. On deuterium-fill shots in low pressure mode, 5.5 mbar, deuterons are accelerated to energies sufficient to cause activation in the graphite target, Fig 3.

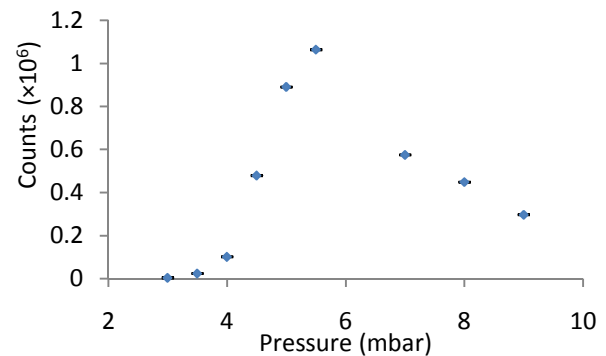


Figure 3. High energy deuteron production in various pressures (error bars indicate statistical errors for yield obtained from series of 30 shots)

It worth noting that the optimum pressure for neutron production in NX2 plasma focus is 14 mbar [13], which is much higher than the optimized pressure for accelerated deuterons. For deuterium filling pressure of 14 mbar, and above, no activation was induced in the target.

The reaction cross section for  $^{12}\text{C}(d, n)^{13}\text{N}$  is shown in Fig 4 [14]. The maximum cross section is 240 mbarns at 2.28 MeV deuteron energy. The experimental results of different plasma focus devices show the highest energy of deuterons is in the range of 1 to 2 MeV [15].

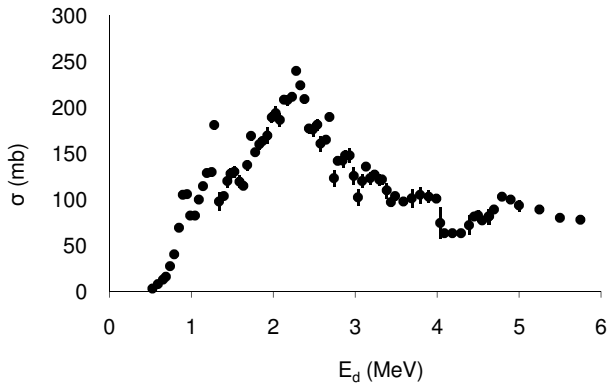


Figure 4. Reaction cross-section for  $^{12}\text{C}(d, n)^{13}\text{N}$

The interaction of high energy deuterons with the graphite target results in the production of Nitrogen-13, which is a short-lived radioisotope and positron decays with the half-life of 9.96 min. The positrons slow down in the graphite and annihilate with electrons. Two oppositely directed 511 keV gamma rays are produced by each positron annihilation event. A BGO scintillation detector and Multi Channel Analyzer (MCA) system are used to detect the 511 keV gamma rays. The major advantages of BGO are its high density ( $7.13 \text{ g cm}^{-3}$ ) and the large atomic number of its bismuth component ( $Z=83$ ). The large  $Z$  results in a high photoelectric absorption of gamma rays. High density results in a large Compton scattering cross section [16].

The efficiency of the BGO and MCA system for 511 keV annihilation gamma ray measurement is obtained by Monte Carlo simulations with MCNPX [17].

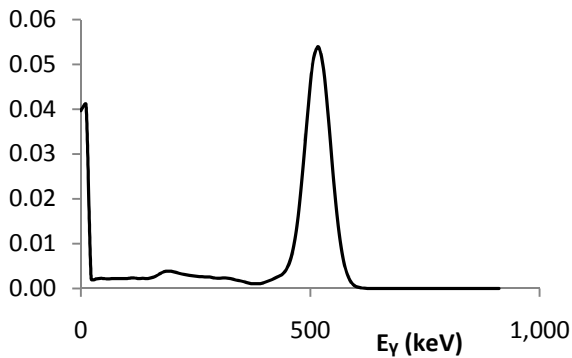


Figure 5. Energy spectrum obtained from MCNP simulation for graphite and BGO geometry

The BGO crystal is cylindrical with a radius of 3" and a thickness of 1". The range of 2 MeV deuterons in graphite is  $24.8 \mu\text{m}$ , so the simulation supposes that the source of positrons is uniformly distributed in a graphite layer of this thickness. Figure 5 shows the energy spectrum from the simulation. The photo peak centered at 511 keV represents annihilation gamma-rays that are completely absorbed in the crystal. Gaussian energy

broadening is used to take account of the energy resolution of the detector. The MCNPX simulations show that the BGO system has an efficiency of 52% for detection of positron annihilation events, using an integration window from 410 to 610 keV.

The thickness of graphite target is 7 mm, which is much greater than the range of the incident deuterons in graphite. Therefore, the number of deuterons incident on the graphite can be estimated using the thick target yield formula [18]:

$$y_t(E_d) = \int_0^R n \sigma(E) dx = n \int_0^{E_d} \frac{\sigma(E)}{|dE/dx|} dE \quad (2)$$

where  $E_d$  is the incident energy of deuterons,  $\sigma(E)$  is the reaction cross section,  $n$  is the target nuclei per  $\text{cm}^3$ ,  $dE/dx$  is the stopping power, and  $R$  is the range of the deuterons in the target. The stopping power is a slowly varying function of energy and was obtained from the SRIM code [19]. Figure 6 displays the calculated thick target yield as a function of deuteron energy.

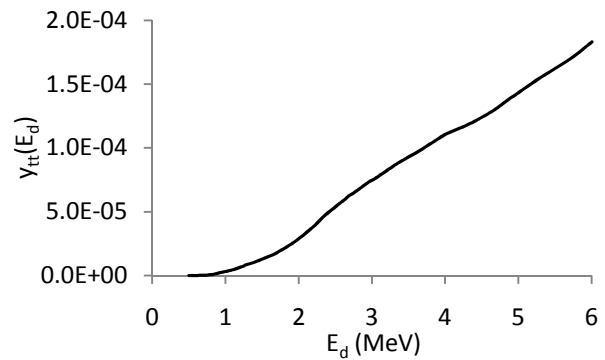


Figure 6. Graphite thick target yield for deuterons

Then the total number of  $^{13}\text{N}$  nuclides produced in the target by deuteron bombardment will be:

$$N_{^{13}\text{N}} = k \int_0^{E_{\text{max}}} E^{-n} y_t(E_d) dE \quad (3)$$

where the deuteron energy distribution follows an empirical power-law of the form:

$$\frac{dn_d}{dE} = kE^{-n} \quad (4)$$

Deuteron spectra of this form have been reported for measurements performed with several other plasma focus devices, generally with  $n \cong 5$  [20,21]. For an  $\sim E^{-5}$  spectrum the distribution of  $^{13}\text{N}$  yield with deuteron energy is shown in Fig 7. Taking  $E_{\text{max}} = 6 \text{ MeV}$  as a practical upper limit, and  $^{13}\text{N}$  yield (at 5.5 mbar) of  $N_{^{13}\text{N}} = 1.90 \times 10^6$ , then the value of  $k$  determined from Eqn. 3 is  $5.95 \times 10^{11} \text{ MeV}^{-1}$ .

Moreover the average number of high energy deuterons,  $E_d > E_{\min}(=0.5 \text{ MeV})$ , responsible for activating the graphite can be estimated from:

$$N_d = k \int_{E_{\min}}^{E_{\max}} E^{-n} dE \quad (5)$$

Giving  $N_d = 2.38 \times 10^{12}$  high energy deuterons per shot. The total energy of these deuterons is calculated from:

$$E_{\text{beam}} = k \int_{E_{\min}}^{E_{\max}} E^{1-n} dE \quad (6)$$

This gives a total energy of 0.25 J, which represents a conversion efficiency of about 0.01% from the stored energy in the capacitors (2.2 kJ) to total beam energy for deuterons above 500 keV.

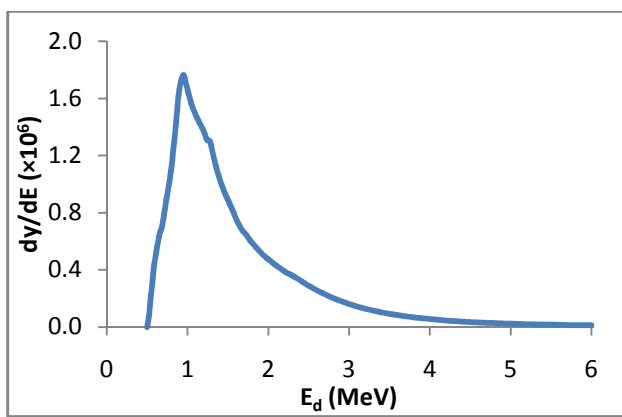


Figure 7. Distribution of reaction yield with deuteron energy for an assumed deuteron energy of the form  $E^{-n}$  (with  $n = 5$ )

#### 4. Conclusion

High energy deuterons ( $>500 \text{ keV}$ ) emitted from plasma focus are investigated by the activation of a graphite target. The relevant reaction is  $^{12}\text{C}(d,n)^{13}\text{N}$ . Nitrogen-13  $\beta^+$  decays leading to the emission of electron-positron annihilation gamma-rays of energy 511 keV. These gamma-rays are measured by a BGO scintillation detector and MCA system. A  $\beta^+$  decay detection efficiency of 52% is determined by MCNPX simulation for the BGO and target geometry. A parametric study shows that the most intense beams of high energy deuterons are produced at 5.5 mbar filling pressure, whereas the optimum pressure for neutron production in the NX2 is 14 mbar. The number of high energy deuterons activating the graphite target is estimated using the calculated thick target yield together with an empirical power-law distribution for the deuteron spectrum of the form  $dn_d/dE = kE^{-5}$ . This gives  $2.38 \times 10^{12}$  deuterons ( $>500 \text{ keV}$ ) per shot. These high energy deuterons possess a total energy of 0.25 J which

represents 0.01% of the capacitor bank energy for the NX2 plasma focus.

#### 5. References

1. R. L. Gullickson, J. S. Luce, H. L. Sahlin, J. Appl. Phys. **48**, 3718 (1977).
2. V. V. Vikhrev, Sov. J. Plasma Physics **12**, 262 (1986).
3. M. J. Bernstein, Physics of Fluids **13**, 2858 (1970).
4. Y. Mizuguchi, J. I. Sakai, H. R. Yousefi, T. Haruki, and K. Masugatab, Phys. Plasmas **14**, 032704 (2007).
5. R. L. Gullickson, H. L. Sahlin, J. Appl. Phys. **49**, 1099 (1978).
6. I. F. Belyaeva, Nucl. Fusion **20**, 1037 (1980).
7. U. Jager, L. Bertalot, H. Herold, Rev. Sci. Instrum. **56**, 77 (1985).
8. G. Gerdin, W. Stygar, F. Venneri, J. Appl. Phys. **52**, 3269 (1981).
9. S. V. Springham, S. Lee, M. S. Rafique, Plasma Phys. Control. Fusion **42**, 1023 (2000).
10. S. Lee. Radiative dense plasma focus model computation package RADPFV5.008. <http://eprints.ictp.it/85/>. 1985.
11. W. E. Bennett, H. T. Richards, Phys. Rev. **71**, 565 (1947).
12. M. J. Bernstein, D. A. Meskan, H. L. L. Van Paassen, Phys. Fluids **12**, 2193 (1969).
13. F. Malik, S. M. Hassan, R. S. Rawat, M. V. Roshan et al., 34<sup>th</sup> ICOPS, Albuquerque, USA. 2007.
14. R. W. Michelmann, J. Krauskopf, J. D. Meyer, K. Bethge, Nuclear Instrum. Methods B. **51**, 1 (1990).
15. F. C. Young, J. Golden, C. A. Kapetanacos, Rev. Sci. Instrum. **48**, 432 (1977).
16. O. Shcherbakov, K. Furutaka, S. Nakamura, H. Harada, K. Kobayashi, Nuclear Instrum. Methods in Phys. Research A. **517**, 269 (2004).
17. MCNPX, Los Alamos National Laboratory. <http://mcnpx.lanl.gov/>.
18. D. B. Cassidy, K. F. Canter, R. E. Shefer, R. E. Klinkowstein, B. J. Hughey, Nuclear Instrum. Methods in Phys. Research B. **195**, 442 (2002).
19. [www.srim.org](http://www.srim.org)
20. L. Bertalot, H. Herold, U Jager, et al, Physics Letters **79A**, 389 (1980).
21. H. Kelly, A. Marquez, Plasma Phys. Control. Fusion **38**, 1931 (1996).